ISSN 1023-1935, Russian Journal of Electrochemistry, 2023, Vol. 59, No. 11, pp. 856–866. © Pleiades Publishing, Ltd., 2023.
Russian Text © The Author(s), 2023, published in Elektrokhimiya, 2023, Vol. 59, No. 11, pp. 674–685.

# Electrochemical Behavior of Dimethyl Sulfone on Platinum Electrode[1]

**M. A. Akhmedov[a, b, *], Sh. Sh. Khidirov[c], and S. I. Suleimanov[a, **]**

[a] *Analytical Center of Collective Use, Dagestan Federal Research Center, Russian Academy of Sciences, Makhachkala, Russia*
[b] *DAGLITHIUM Limited Liability Company, Makhachkala, Russia*
[c] *Dagestan State University, Makhachkala, Russia*
**e-mail: muhamadahmedov@mail.ru*
***e-mail: khidirovdgu@mail.ru*

Received November 30, 2022; revised March 15, 2023; accepted May 4, 2023

**Abstract**—The effect of dimethyl sulfone ($DMSO_2$) on the rates of anodic oxygen evolution and cathodic hydrogen evolution on the platinum electrode in acidic and alkaline media is studied. Quantum chemical calculations on the theoretical level PBE/def2-TZVP show that in the dimethyl sulfone molecule, the break of the C–S bond is preferred over the C–H bond break and the process itself proceeds by the radical-ion mechanism. The NMR and Raman spectroscopic studies show that the final products of the anodic oxidation of dimethyl sulfone are methanesulfonic acid and dimethyldisulfone in the acidic medium and only dimethyldisulfone in the alkaline medium. The final products of the cathodic reduction of $DMSO_2$ are dimethylpolysulfides. Based on experimental results, a scheme of the electrocatalytic behavior of dimethyl sulfone of the platinum electrode is proposed.

**Keywords:** dimethyl sulfone, dimethyl disulfone, dimethyl polysulfides, kinetics, methanesulfonic acid, platinum, electrooxidation, electroreduction, electrolysis

**DOI:** 10.1134/S1023193523110034

## INTRODUCTION

Nowadays, keen attention is drawn to the selective and ecologically safe methods of functionalization of various organic compounds using electrocatalytic processes [1–3]. The recent achievements showed that the bonds carbon–carbon and carbon–heteroatom (C–S, C–N, etc.) can be formed by electrochemical cross dehydrogenation [4–6]. From the standpoint of the ecologically-friendly strategy, the use of electrocatalytic processes in the modern organic synthesis is a reliable approach that allows synthesizing compounds unavailable by chemical methods and without using toxic oxidants or reducers [7, 8].

Furthermore, of special interest are the electrode processes on platinum (Pt), because the latter is a unique low-temperature electrocatalyst [9–11] that exhibits anodic stability and corrosion resistance to oxidants and also can selectively polarize, oxidize or reduce functional groups in organic molecules leaving untouched the remaining part [12–14].

In [15], the method of voltammetry of immobilized microparticles (VIMP) was proposed as a diagnostic criterion of the electrochemical oxidation/reduction of organosulfur compounds which allowed analyzing the vast analytical information on poorly soluble organosulfur compounds contained in the asphalt-concrete road covering. The method is based on measuring voltammetric responses of a solid that is attached mechanically to the surface of a porous inert electrode (usually graphite electrode impregnated with kerosene) in contact with a suitable electrolyte.

The study object, dimethyl sulfone ($DMSO_2$), due to its high permittivity and electrochemical stability (in nonaqueous media) can dissolve sufficiently well salts of many metals by almost ionizing them [16, 17] and, hence, is widely used in different electrochemical applications [18–21].

In [22–24], for synthesizing thiosulfonates and aromatic sulfones, a series of methods of electrochemical C–S coupling were considered, in which halides of metals and ammonium were used as the supporting electrolytes and redox catalysts.

The authors of [25] reported on the selective oxidation of diarylsulfides and arylalkylsulfides to the corre-

[1] Delivered at the 20th All-Russian Meeting "Electrochemistry of Organic Compounds" (EKhOS-2022), Novocherkassk, October 18–22, 2022.

sponding sulfoxides and sulfones under electrochemical conditions, where sulfoxides were formed at the current of the order of magnitude of 5 mA, whereas sulfones were the main products at 10–20 mA in MeOH. In [26], it was noted that in nonaqueous media, the sulfur-containing depolarizer itself can take part in the electrode process.

It is known that the electrooxidation of dimethyl sulfone produces dimethyl disulfone in alkaline medium [27, 28] and methanesulfonic acids and dimethyl disulfone in acidic medium [29–32]. The cathodic reduction of dimethyl sulfone in acidic medium produces dimethyl polysulfides. It is shown [33] that on the Pt electrode surface, $DMSO_2$ forms stronger adsorption bonds as compared with hydrogen- and oxygen-containing species.

In this study, we considered the kinetics of dimethyl sulfone electrooxidation on the Pt electrode in a wide potential region and also showed for the first time the results of quantum-chemical calculations aimed at elucidation of the possible routes of anodic oxidation and cathodic reduction of dimethyl sulfone of the Pt electrode.

## EXPERIMENTAL

The following reagents were used without preliminary cleaning: dimethyl sulfone $CH_3S(O)_2CH_3$ (Sigma Aldrich), sulfuric acid (special grade), and sodium hydroxide (reagent grade).

As the supporting electrolyte, we used 0.1 M solutions of sulfuric acid ($H_2SO_4$) and sodium hydroxide (NaOH). Solutions were prepared using twice distilled deionized water.

The electrochemical studies were carried out in a three-electrode electrochemical cell with anodic and cathodic compartments separated by a fitted-in ceramic diaphragm. The volt-ampere measurements were carried out at temperature of 20 ± 2°C using an automatic potentiostat-galvanostat IPC-Pro MF (Volta, Russia). The potential was measured with respect to the reversible hydrogen electrode (RHE) in 1.0 M $H_2SO_4$. Hydrogen of the 99.9999% purity was produced by a HGP-6 generator (Khimelektronika, Russia). The reference electrode was brought closely to the working electrode surface by means of an electrolytic bridge and a Luggin capillary filled with the working solution. The working solution in the cell was blown though by inert gas (argon). Polycrystalline platinum with the geometrical surface of 0.016 $cm^2$ was used as the working electrode; its true surface determined by the method of [14] was 0.02 $cm^2$. The counter electrode was a platinum plate.

When measuring stationary polarization curves, the working electrode was exposed at each potential for 15–60 min until the current stopped to change.

The kinetic relationships were found by analyzing the stationary polarization curves in coordinates η vs. log (*j*) to determine their tangent (*b*) and the Tafel equation parameters Eqs. (1)–(3)

$$\eta = a + b\log|j_0|, \quad (1)$$

$$a = -\frac{RT}{\alpha zF}\ln j_0, \quad (2)$$

$$b = \frac{2.3RT}{\alpha zF}, \quad (3)$$

where η, the activation barrier (overpotential) for the electrochemical reaction, was found from Eq. (4) as the difference between the electrode potential (*E*, V) and the equilibrium potential ($E_{eq}$, V)

$$\eta = E - E_{eq}, \quad (4)$$

*a* is the constant determined by the nature of electrode material; $j_0$ is the exchange current ($A/m^2$ or $mA/cm^2$); α is the charge transfer coefficient for the cathodic (β—for anodic) reaction which characterizes the contribution made by the electric field of the electric double layer (EDL); *z* is the number of electrons involved in the electrode reaction; *F* is the Faraday constant (96 500 C/mol = 26.8 A h); *R* is the universal gas constant (8.315 J/(mol K); *T* is the absolute temperature (K).

By extrapolating the linear segments of polarization curves to η = 0, the exchange current $j_0$ was determined [35]. The exchange current density ($j_0$) in the equation of Butler–Volmer (5) characterizes the rate constant of the electrode reaction at the equilibrium potential:

$$j = j_0\left[\exp\left(-\frac{\alpha zF\eta}{RT}\right) - \exp\left(\frac{(1-\alpha)zF\eta}{RT}\right)\right], \quad (5)$$

when the cathodic overpotential of the electrochemical reaction exceeds (Eq. (6)) the anodic overpotential, the Bulter–Volmer equation [36] coincides with the Tafel equation and takes the following form (Eq. (7)):

$$\eta_k \gg \frac{RT}{zF}, \quad (6)$$

$$\eta_k = -\frac{RT}{\alpha zF}\ln j_0 + \frac{RT}{\alpha zF}\ln j_k. \quad (7)$$

The preparative electrolysis was carried out on platinum electrodes with the geometrical surface of 0.25 $cm^2$ in a diaphragm electrolyzer at the controlled current density for 32 h using a dc rectifier TYPE:TR-9252. The corresponding current densities of oxidation/reduction of $DMSO_2$ were determined based on the stationary anodic/cathodic voltammograms. A perfluorinated cation-exchange membrane MF-4SK (Plastomer, Russia) was used as the diaphragm. At the stationary electrolysis, the temperature was maintained in the interval of 25–30°C.

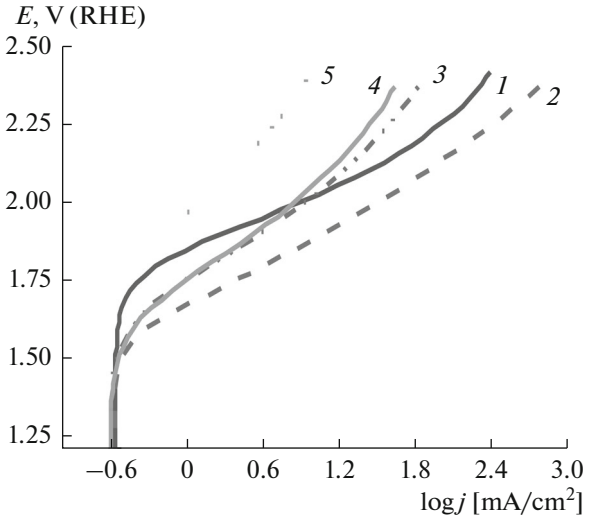


**Fig. 1.** Anodic voltammograms of Pt electrode measured in the stationary mode in (*1*) 0.1 M $H_2SO_4$ and in the presence of $DMSO_2$, M: (*2*) 0.1; (*3*) 0.2; (*4*) 0.4; (*5*) 0.8.

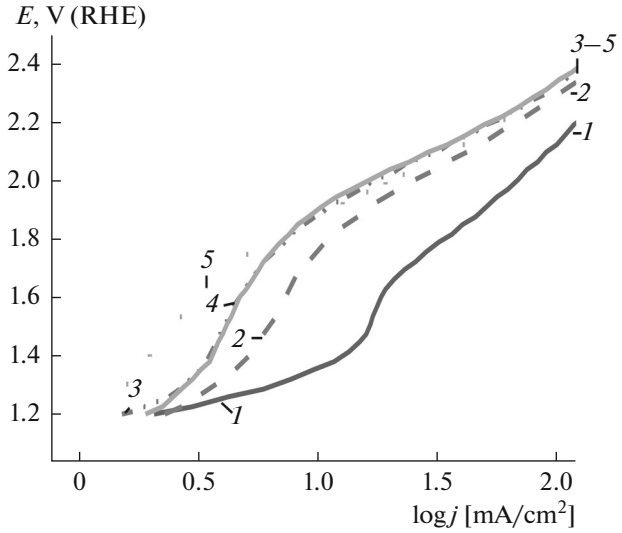


**Fig. 2.** Anodic voltammograms of Pt electrode measured in the stationary mode in (*1*) 0.1 M NaOH and in the presence of $DMSO_2$, M: (*2*) 0.1; (*3*) 0.2; (*4*) 0.4; (*5*) 0.8.

To measure Raman spectra, the analyzed sample was placed in a quartz ampoule, which was first evacuated using a vacuum pump and then filled with argon and sealed. The Raman spectra of samples before and after electrolysis were measured using a spectrometer DXR Smart Raman Research (Thermo Scientific, United States) with laser excitation ($\lambda$ = 532 nm and power of 10 mW), the spectrum range was 50–3500 $cm^{-1}$ with resolution of 3–5 $cm^{-1}$, the integration time was 20 s for each scan.

The 3D models of molecular structures were obtained using program ACD/Labs Freeware 2015. After this, their preliminary geometrical optimization was carried out by the DFT method at the level B97-3c [37] using the program Orca 4.2.0 [38, 39]. The final calculations of the electronic structure (with the complete geometrical optimization) and the energy characteristics were carried out by the simplified method of generalized gradient approximation (PBE) with polarized triply split basis set of wave functions (def2-TZVP) by taking into account the spin multiplex character of the molecular and atomic radical species; the effect of the aqueous medium was taken into account using the polarized continuum model (CPCM) [40–43].

## RESULTS AND DISCUSSION

### *Electrooxidation of Dimethyl Sulfone*

The anodic voltammograms measured on a Pt electrode under stationary conditions in 0.1 M $H_2SO_4$ (Fig. 1) and 0.1 M NaOH (Fig. 2) as the supporting electrolytes with and without addition of $DMSO_2$ in different concentrations demonstrated a rise of the current at the potential above 1.1 V (RHE) which was associated with the formation and evolution of oxygen (Eqs. (8) and (9)) [33].

$$\text{In acidic medium: } 2H_2O \rightarrow O_2 + 4H^+ + 4\bar{e}, \quad E \geq 1.2 \text{ V (RHE)}, \tag{8}$$

$$\text{in alkaline medium: } 4HO^- \rightarrow O_2 + 2H_2O + 4\bar{e}, \quad E \geq 0.4 \text{ V (RHE)}. \tag{9}$$

The anodic voltammograms (Fig. 1) measured on the Pt electrode in aqueous 0.1 M solutions of $H_2SO_4$ with addition of $DMSO_2$ showed that the overpotential of oxygen evolution increased at the $DMSO_2$ concentration higher than 0.1 M. The similar effect was observed in 0.1 M NaOH solution in the presence of $DMSO_2$ (but for all concentrations studied) (Fig. 2).

The decrease in the current observed in anodic curves *3–5* (Fig. 1) in the presence of different concentrations of $DMSO_2$ was associated with suppression of the oxygen evolution reaction (Eq. (6)), with the exception of curve *2*. In the latter case, the oxidation current of the oxygen reaction in the presence of 0.1 M $DMSO_2$ was higher as compared with curve *1* measured in the supporting electrolyte, i.e., 0.1 M $H_2SO_4$. This could be associated either with the oxidation of dimethyl sulfone molecules or with the contribution made by the heterogeneous surface of the platinum electrode to the increase in the current density in the presence of 0.1 M $DMSO_2$.

It deserves mention that the surface of the Pt electrode in aqueous solutions at the anodic potentials was covered by various chemisorbed oxygen-containing species [44, 45].

**Table 1.** Tafel coefficients $a$, $b$, and β for Pt electrode in the potential interval of 1.8–2.1 V (RHE) and the exchange current $j_0$ of the oxygen reaction (Eq. (6)) in 0.1 M $H_2SO_4$ with and without addition of $DMSO_2$

| $C$ ($DMSO_2$), M | $a$ | $b$ | $R^2$ | $j_0$, mA/cm$^2$ | β |
|---|---|---|---|---|---|
| 0 | 0.68 ± 0.03 | 0.19 ± 0.01 | 0.99 | 0.002 | 0.31 |
| 0.1 | 0.68 ± 0.03 | 0.23 ± 0.01 | 0.99 | 0.01 | 0.26 |
| 0.2 | 0.68 ± 0.03 | 0.27 ± 0.01 | 0.99 | 0.02 | 0.23 |
| 0.4 | 0.68 ± 0.03 | 0.31 ± 0.01 | 0.99 | 0.05 | 0.19 |
| 0.8 | 0.68 ± 0.03 | 0.38 ± 0.02 | 0.98 | 0.14 | 0.15 |

**Table 2.** Tafel coefficients $a$, $b$, and β for Pt electrode in the potential interval of 1.8–2.1 V (RHE) and the exchange current $j_0$ of the oxygen reaction (Eq. (7)) in 0.1 M NaOH with and without addition of $DMSO_2$

| C ($DMSO_2$), M | $a$ | $b$ | $R^2$ | $j_0$, mA/cm$^2$ | β |
|---|---|---|---|---|---|
| 0 | 0.22 ± 0.02 | 0.76 ± 0.01 | 0.99 | 1.16 | 0.31 |
| 0.1 | 0.22 ± 0.02 | 0.75 ± 0.03 | 0.98 | 1.15 | 0.32 |
| 0.2 | 0.22 ± 0.02 | 0.64 ± 0.03 | 0.98 | 1.02 | 0.37 |
| 0.4 | 0.23 ± 0.03 | 0.56 ± 0.04 | 0.97 | 0.89 | 0.42 |
| 0.8 | 0.23 ± 0.03 | 0.45 ± 0.03 | 0.97 | 0.71 | 0.52 |

Based on the linear segments in anodic voltammograms (Figs. 1 and 2) at 1.7–2.1 V (RHE), the Tafel equation coefficients were determined (Tables 1 and 2).

According to Table 1 and 2, in the linear interval of 1.8–2.1 V (RHE) the open-circuit potential (coefficient $a$) was independent of the dimethyl sulfone concentration. The different values of the tangent ($b$) and the exchange current ($j_0$) of oxygen evolution observed in acidic and alkaline media pointed to the different mechanisms of dimethyl sulfone oxidation. The change of the transfer coefficient $\beta \le 0.5$ was associated with the fact that the electrode reaction was asymmetric and proceeded irreversibly in the anodic direction.

The calculated exchange currents (Table 1) correlated with the data of [46, 47]. At the same time, it should be noted that the charge transfer coefficient and the exchange current for the hydrogen evolution on platinum depended on several factors, namely, the pH of the medium, the electrolyte composition and concentration.

It follows from Tables 1 and 2 that dimethyl sulfone exerted a considerable effect on the oxygen evolution rate in acidic and alkaline media. Thus, in the alkaline medium, as the $DMSO_2$ concentration increased, the anodic oxygen evolution rate noticeably decreased, whereas in the acidic medium, the rate increased. We assumed that these differences may be associated with the different mechanism of electrochemical oxidation of dimethyl sulfone in acidic and alkaline media.

The quantum-chemical calculations by the method of generalized gradient approximation with polarized triply split basis set of wave functions (PBE/def2-TZVP) showed that in the dimethyl sulfone molecule, the break of the C–S bond is more advantageous (Table 3) as compared with the C–H bond.

According to [48], the break of the HO–H bond in the water molecule requires about 118.8 kcal/mol (497.1 kJ/mol) in vacuum. The calculations of the dissociation energy of water molecule shown in Table 3 took into account the effect of the solvent (water) according to CPCM [43].

From the calculated changes in the Gibbs energy ($\Delta G$, kJ/mol) of bond formation for possible recombination reactions of dimethysulfone species, which were also determined by the DFT method (Table 4), it is seen that the highest $\Delta G$ corresponds to the interaction of methylsulfo groups ($CH_3S\bullet(O)_2$) with OH radicals to form methanesulfonic acid.

**Table 3.** Bond breaking energy in water and dimethyl sulfone molecules

| No. | A → B | $\Delta E$, $E_h$ | $\Delta E$, kJ/mol |
|---|---|---|---|
| 1 | $2H_2O \rightarrow OH^- + H_3O^+$ | 0.119 | 313.301 |
| 2 | $CH_3S(O)_2CH_3 \rightarrow CH_3SO_2\bullet + \bullet CH_3$ | 0.120 | 315.212 |
| 3 | $CH_3S(O)_2CH_3 \rightarrow CH_3SO_2CH_2\bullet + \bullet H$ | 0.185 | 486.943 |

**Table 4.** The changes in the Gibbs energy in possible recombination reactions of dimethyl sulfone species

| No. | A → B | $\Delta G$, $E_h$ | $\Delta G$, kJ/mol |
|---|---|---|---|
| 1 | $CH_3S\bullet(O)_2\bullet + \bullet OH \rightarrow CH_3{-}S(O)_2{-}OH$ | −0.106 | −278.915 |
| 2 | $2CH_3S\bullet(O)_2\bullet \rightarrow CH_3{-}S(O)_2{-}S(O)_2{-}CH_3$ | −0.021 | −56.345 |
| 3 | $2CH_3S(O)_2CH_2\bullet + \bullet S(O)_2CH_3\bullet \rightarrow CH_3S(O)_2CH_2S(O)_2CH_3$ | −0.0596 | −156.545 |
| 4 | $2CH_3S(O)_2CH_2\bullet \rightarrow CH_3S(O)_2CH_2CH_2S(O)_2CH_3$ | −0.103 | −269.414 |

Were the C–H bond broken, then derivatives 3 and 4 would be formed from the dimethyl sulfone molecule (Table 4). The low $\Delta G$ of dimethyl sulfone ($CH_3{-}S(O)_2{-}S(O)_2{-}CH_3$) indicates that this substance is unstable and can undergo further transformations.

The analysis of NMR (Fig. 5) and Raman (Fig. 6) spectra of the final products of dimethyl sulfone electrolysis formed in the anodic compartment of a diaphragm electrolyzer at the current density of 0.01–0.03 A/cm$^2$ confirmed only the formation of derivatives 1 and 2 (Table 4).

The $^1$H-NMR spectrum (500 MHz, DMSO-$d_6$) of original $DMSO_2$ demonstrated the following chemical shifts (δ), ppm: 3.34($^1$H, CH doublet), 3.13 ($^1$H, $CH_3$ doublet), 2.99 ($^5$H, $CH_3$ singlet). The $^1$H-NMR spectrum (500 MHz, DSO-$d_6$) of the oxidation product of $DMSO_2$ (Fig. 3, spectrum *2*) demonstrated the following chemical shifts (δ), ppm: 3.33 ($^1$H, CH singlet), 2.98 ($^5$H, $CH_3$ singlet). The $^1$H-NMR spectrum (500 MHz, DMSO-$d_6$) of the second oxidation product of $DMSO_2$ (Fig. 3, spectrum *3*) demonstrated the chemical shifts (δ), ppm: 2.38 ($^3$H, $CH_3$ singlet); 8.38 ($^1$H, OH singlet). The information on chemical shifts makes it possible to assess the changes in the structure of the final product.

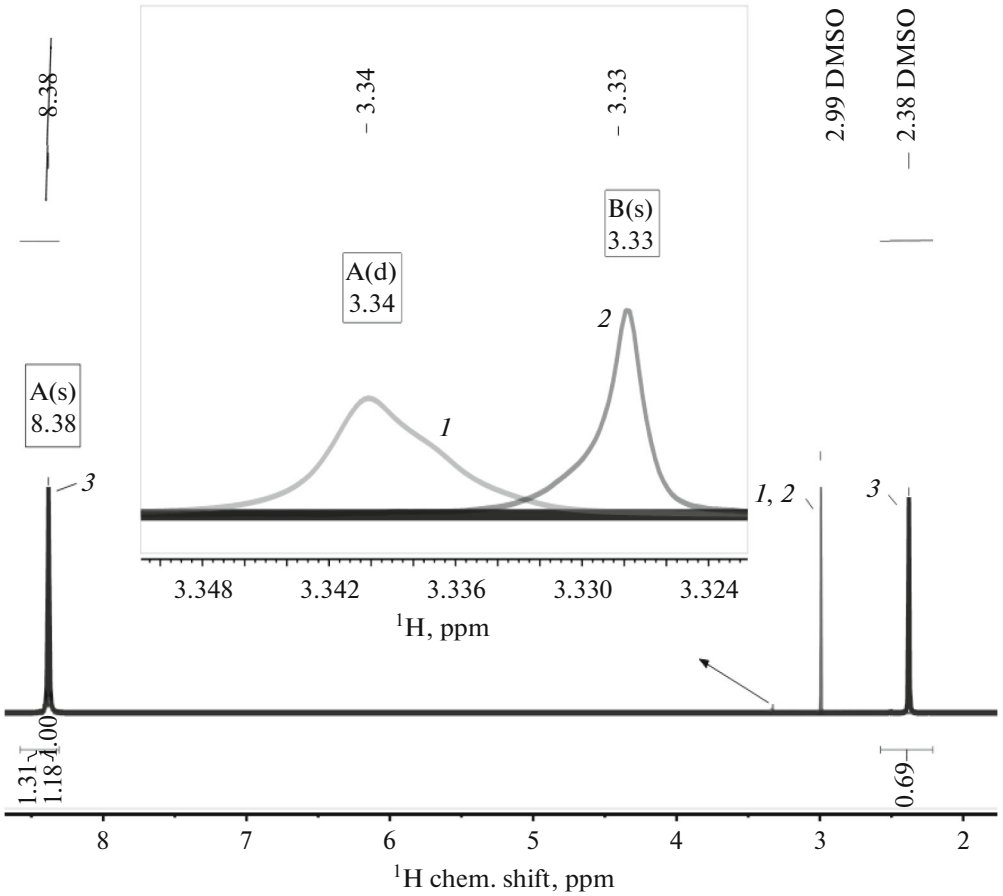


**Fig. 3.** $^1$H-NMR spectra of (*1*) $DMSO_2$ and its electrooxidation products: (*2*) dimethyldisulfone and (*3*) methanesulfonic acid, in the presence of solvent DMSO-$d_6$ = 2 : 1 (vol.), $T$ = 22.8°C.

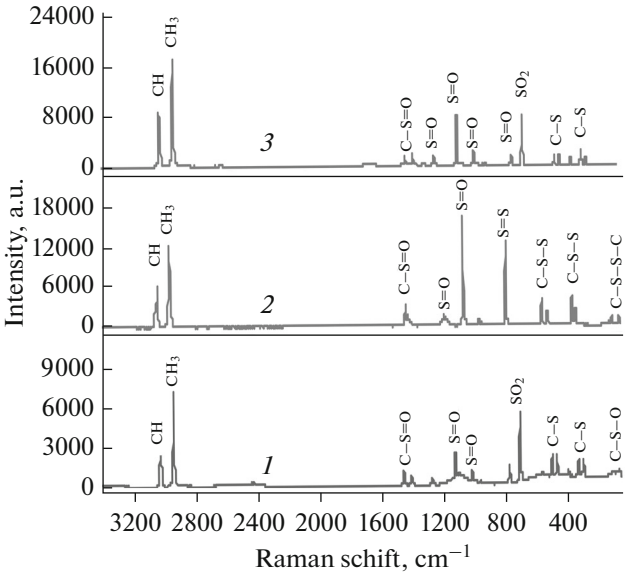


**Fig. 4.** Raman spectra of (*1*) $DMSO_2$ and final products of its electrooxidation: (*2*) dimethydisiulfone and (*3*) methanesulfonic acid.

It should be noted that the presence of electron-withdrawing groups such as S–S and S–O near protons could descreen the latter, i.e., pull off the electron density from protons and shift their signals to the weaker field (δ) [49]. Figure 3 shows the differences between $^1$H chemical shifts in NMR spectra *1* and *2* observed both in the weak (by 0.01 ppm) and strong fields (by 8.38 ppm). Apparently, this can be associated with the presence of the disulfone group which simultaneously contains electron-withdrawing (oxygen (O)) and electron-donating (sulfur (S)) nuclei.

Thus, the comparative analysis of $^1$H-NMR spectra (Fig. 3) of initial and final products after the electrolysis of 0.2 M $DMSO_2$ in acidic medium showed that the difference between the $^1$H-NMR spectra *1* and *3* (the change in the weak field by 0.1 ppm) was associated with the presence of the $S(O)_2S(O)_2$ group that simultaneously contains electron-withdrawing (oxygen O) and electron-donating (sulfur S) nuclei, which corresponds to the molecular form of dimethyl sulfone.

The qualitative difference between the functional groups in the dimethyl sulfone electrooxidation products was also observed in Raman spectra (Fig. 4) in the "fingerprint" region (1600–100 cm$^{-1}$).

Thus, based on the results of quantum-chemical calculations is was assumed that the rise of curve *2* (Fig. 1) was associated with the electrooxidation of dimethyl sulfone in acidic medium at the concentration $C_{DMSO_2} \le 0.1$ M which can occur as a result of the break of C–S bond followed by the formation of methanesulfonic acid (10)–(13).

$$H_3C-\overset{\overset{O}{\|}}{\underset{\underset{O}{\|}}{S}}-CH_3 \longrightarrow H_3C-\overset{\overset{O}{\|}}{\underset{\underset{O}{\|}}{S^{\bullet}}} + CH_3^{\bullet}, \quad (10)$$

$$Pt-OH \longrightarrow Pt^{\bullet} + HO^{\bullet}, \quad (11)$$

$$Pt^{\bullet} + CH_3^{\bullet} \longrightarrow Pt-CH_3, \quad (12)$$

$$H_3C-\overset{\overset{O}{\|}}{\underset{\underset{O}{\|}}{S^{\bullet}}} + HO^{\bullet} \longrightarrow H_3C-\overset{\overset{O}{\|}}{\underset{\underset{O}{\|}}{S}}-OH. \quad (13)$$

The current drop in curves *3–5* (Fig. 1) can be associated with the displacement of OH species from the platinum surface and the adsorption of a large number of dimethyl sulfone molecules. The formed methylsulfone groups dimerized by reaction (14) to form dimethyl sulfone.

$$2H_3C-\overset{\overset{O}{\|}}{\underset{\underset{O}{\|}}{S^{\bullet}}} \longrightarrow H_3C-\overset{\overset{O}{\|}}{\underset{\underset{O}{\|}}{S}}-\overset{\overset{O}{\|}}{\underset{\underset{O}{\|}}{S}}-CH_3. \quad (14)$$

The methyl radical can be oxidized by the one-electron mechanism in which one electron passes to the oxygen atom or some other oxidant. For example, the reaction of the methyl radical with the oxygen molecule ($O_2$) produces the methylperoxide radical ($CH_3OO\cdot$). In this reaction, the methyl radical is oxidized to the oxidation state +1, and one of oxygen atoms in the $O_2$ molecule decreases its oxidation state from 0 to −1/2. Such one-electron processes play the important role in biochemical reactions and fuel combustion processes. The methylperoxide radical is a very active unstable species that decomposes to various products [50]. Formaldehyde can be one of intermediate products of methyl radical oxidation. At the same time, the role of oxidant can be played by the oxygen species chemisorbed on the platinum surface, which are strong oxidants in the vicinity of 1.8 V (RHE) [44, 45]. These assumptions can be confirmed or rejected by carrying out the EPR analysis.

It was noted [51, 52] that methyl radicals are reduced sufficiently easily even in the region of relatively low anodic potentials. At the same time, the C–S bond break and oxidation in the $DMSO_2$ molecule in the acidic medium can proceed at the higher anodic potential of 1.8 V (RHE).

In the alkaline medium, the main product of dimethyl sulfone electrooxidation at the current density of 0.01–0.02 A/cm$^2$ was dimethyldisulfone irrespective of the dimethyl sulfone concentration. We assumed that the C–S break in the $DMSO_2$ molecule in 0.1 M NaOH occurred at the higher anodic poten-

**Table 5.** Tafel equation coefficients $a$, $b$, and α on Pt electrode in the cathodic potential region of –0.2...–0.6 V (RHE) and the exchange current $j_0$ for the hydrogen ion electroreduction in 1.0 M $H_2SO_4$ solution with and without $DMSO_2$

| $C(DMSO_2)$, M | $a$ | $b$ | $R^2$ | $j_0$, mA/cm$^2$ | α |
|---|---|---|---|---|---|
| 0.000 | 0.68 ± 0.02 | 0.71 ± 0.01 | 0.99 | 0.11 | 0.04 |
| 0.001 | 0.68 ± 0.02 | 0.66 ± 0.01 | 0.99 | 0.09 | 0.04 |
| 0.010 | 0.68 ± 0.02 | 0.57 ± 0.01 | 0.99 | 0.06 | 0.03 |
| 0.050 | 0.68 ± 0.02 | 0.43 ± 0.03 | 0.97 | 0.03 | 0.03 |
| 0.100 | 0.68 ± 0.02 | 0.41 ± 0.03 | 0.97 | 0.02 | 0.02 |

tial of 1.8 V (RHE), where, in the absence of OH species on the platinum electrode surface and at the suppressed oxygen evolution, the reaction of dimerization of methylsulfo groups prevailed.

### *Electroreduction of Dimethyl Sulfone*

The rise of the cathodic current at the potential above 0.1 V (RHE) in voltamograms of Pt electrode (Fig. 5) measured under stationary conditions in 1.0 M $H_2SO_4$ solutions with addition of $DMSO_2$ corresponded to formation and evolution of hydrogen Eq. (15).

$$2H^+ + 2\bar{e} \rightarrow H_2. \quad (15)$$

In the cathodic potential region of –(0.2–0.6) V, based on the linear segments in curves *1*–*6* (Fig. 5),

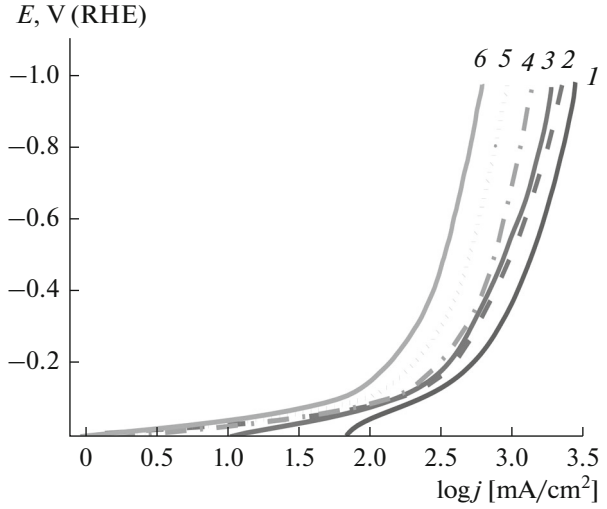


**Fig. 5.** Stationary voltammograms of Pt electrode in (*1*) 1.0 M $H_2SO_4$ and with addition of $DMSO_2$, M: (*2*) 0.001; (*3*) 0.01; (*4*) 0.05; (*5*) 0.1.

the Tafel equation coefficients were determined (Table 3).

The $DMSO_2$ concentration had no effect on the variation of the open-circuit potential on the Pt electrode, whereas the decrease in $j_0$ characterized the decrease in the rate of hydrogen evolution (Table 5). The changes in the coefficient α can probably be associated with the cathodic reduction of $DMSO_2$ on the Pt surface. The Tafel coefficients and the exchange current (Table 5) adequately agreed with the literature data [53–55].

To find the composition of the $DMSO_2$ reduction products formed in the cathodic compartment of the diaphragm electrolyzer, the preparative electrolysis was carried out at a current density of 0.1 A/cm$^2$. After its completion (in 16 h), a black film coating oxidizable in air was observed on the Pt cathode surface.

The electrolysis product was analyzed by the NMR and Raman techniques.

The NMR analysis (Fig.6) was carried out in the presence of solvents (DMSO-$d_6$ and $CDCl_3$). The $^1$H-NMR spectrum (500 MHz, DMSO-d6) of the original $DMSO_2$ (Fig. 6, spectrum *1*) demonstrated the chemical shifts (δ), ppm: 3.34 ($^1$H, $CH_3$ doublet), 3.13 ($^3$H, $CH_3S$ doublet), 2.99 ($^5$H, $CH_3$ singlet), 2.50 ($^6$H, $CH_3$ singlet). The $^1$H-NMR spectrum (500 MHz, $CDCl_3$) of the $DMSO_2$ electroreduction product (Fig. 6, spectrum *2*) demonstrated the following chemical shifts (δ), ppm: 3.33 ($^1$H, CH singlet), 2.99 ($^5$H, $CH_3$ singlet), 2.53 ($^6$H, $CH_3$ singlet), 2.25 ($^3$H, $CH_3$ singlet), 1.76 ($^1$H, CH singlet). According to the reference data [49], for this composition, the chemical shifts of proton nuclei in the strong field in NMR spectra (Fig. 6) can be associated with the electron-donating S–S groups [49].

The $DMSO_2$ electroreduction product was also studied by the Raman spectroscopy. The characteris-

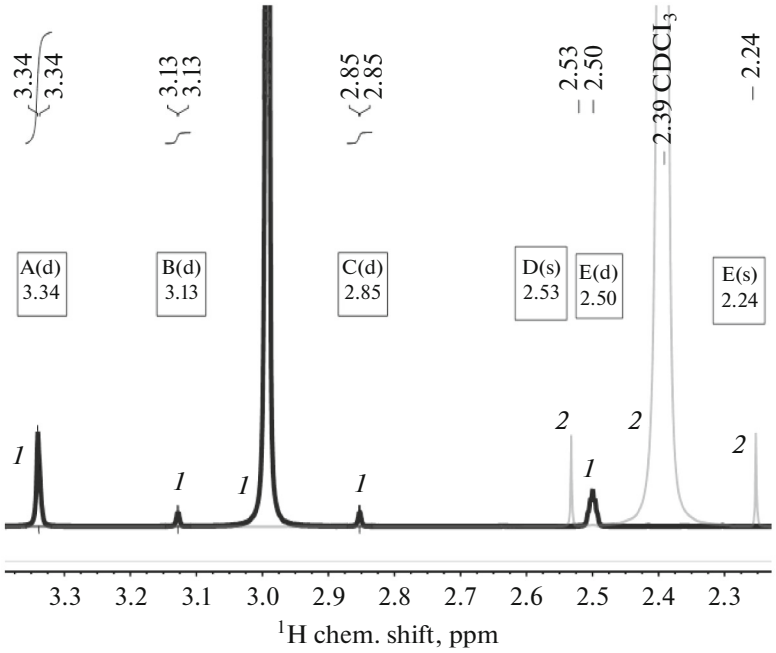


**Fig. 6.** $^1$H-NMR spectra of (*1*) $DMSO_2$ and (*2*) its electroreduction product in the presence of solvents DMSO-$d_6$ and $CDCl_3$ = 2 : 1 (vol), $T = 22.8°C$.

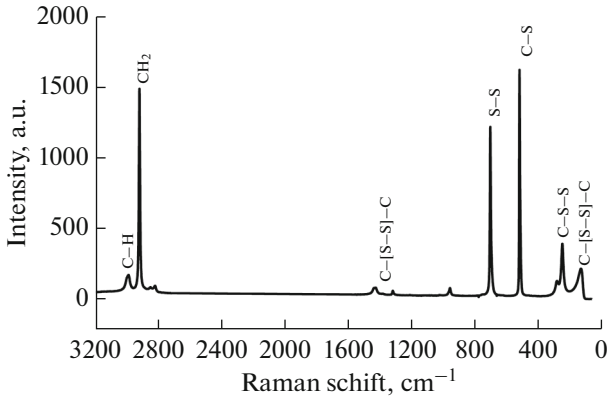


**Fig. 7.** Raman spectra of the reaction product detached from the Pt cathode surface after the electrolysis of $DMSO_2$ in 1.0 M $H_2SO_4$.

tic bands of deformational vibrations for S—S bonds appeared in Raman spectra (Fig. 7) at 693 and 119 $cm^{-1}$.

Based on the results of analysis, it was shown that the methylsulfone electroreduction in the acidic medium produced dimetyl polysulfide. The following mechanism was proposed for the cathodic reduction:

$$Pt-\overset{\overset{O}{\|}}{\underset{\underset{O}{\|}}{S}}-CH_3 + 4\bar{e} + 4H^+ \rightarrow Pt-S-CH_3 + 2H_2O, \quad (16)$$

$$2Pt{-}S{-}CH_3 \rightarrow CH_3{-}S{-}S{-}CH_3 + 2Pt, \quad (17)$$

$$n CH_3{-}S{-}S{-}CH_3 + n\bar{e} \rightarrow n\left[CH_3{-}(S{-}S)_{n+2}{-}CH_3\right] + nC_2H_6. \quad (18)$$

Based on experimental data obtained in this study, the generalized scheme (Fig. 8) of the electrochemical behavior of dimethyl sulfone on the Pt electrode in alkaline media was proposed.

## CONCLUSIONS

Based on the found kinetic parameters, it is shown that as the concentration of dimethyl sulfone in acidic and alkaline media decreases, the rates of anodic oxygen evolution and cathodic hydrogen evolution on the platinum electrode decrease. The quantum chemical calculation has shown that in the dimethyl sulfone molecule, the break of the C–S bond is more advantageous as regards energy as compared with the C–H bond. It is assumed that the electrooxidation and electroreduction of $DMSO_2$ proceeds by the radical-ion mechanism. The changes in the transfer coefficients $\alpha$ and $\beta$ for reactions of hydrogen and oxygen evolution, respectively, may be associated with irreversibility of the processes of dimethyl sulfone electroreduction and electrooxidation on the Pt electrode. The results of NMR and Raman spectroscopic studies confirm that the final products of the dimethyl sulfone anodic oxidation in acidic medium are methanesulfonic acid and dimethyl disulfone; in alkaline medium, only dimethyldisulfone is formed. At the same time, the cathodic reduction product of $DMSO_2$ is dimetyl polysulfide. A

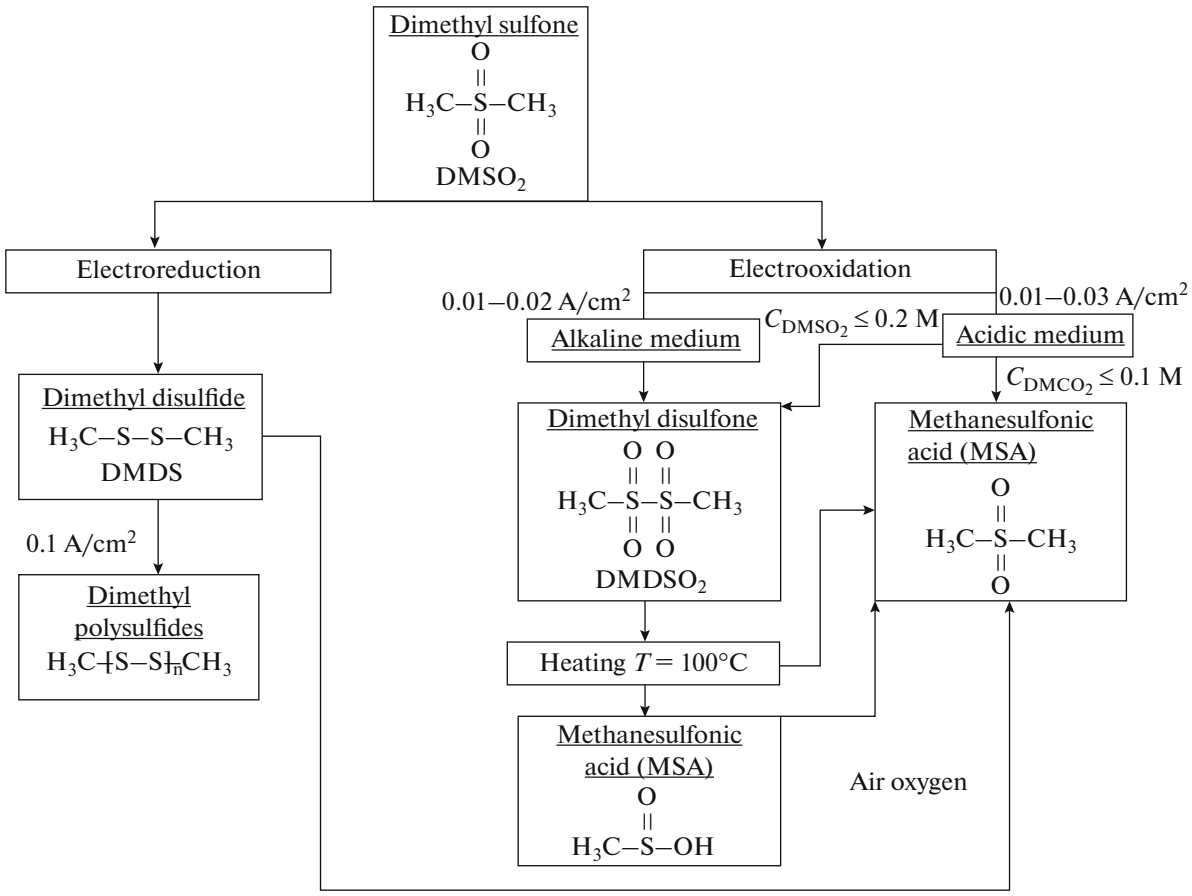


**Fig. 8.** Scheme of the electrochemical behavior of dimethyl sulfone on Pt electrode.

scheme of the electrochemical behavior of dimethyl sulfone on the platinum electrode is proposed.

## ACKNOWLEDGMENTS

The study was carried out using instruments of the Analytical Center of Collective Use of the Dagestan Federal Research Center of the Russian Academy of Sciences.

## FUNDING

This study was financially supported by the Foundation to Promote Innovations (grant no. 4470GS1/72582 from February 15, 2022 (S1-112576)).

## CONFLICT OF INTEREST

The authors declare that they have no conflict of interest.

## REFERENCES

1. Budnikova, Y.H., Electrochemical insight into mechanisms and metallocyclic intermediates of C–H functionalization, *Chem. Record*, 2021, vol. 21, no. 9, p. 2148. https://doi.org/10.1002/tcr.202100009
2. Lyalin, B.V., Sigacheva, V.L., Kudinova, A.S., Neverov, S.V., Kokorekin, V.A., and Petrosyan, V.A., Electrooxidation is a promising approach to functionalization of pyrazole-type compounds, *Molecules*, 2021, vol. 26, no. 16, p. 4749. https://doi.org/10.3390/molecules26164749
3. Akulov, A.A., Varaksin, M.V., Charushin, V.N., and Chupakhin, O.N., C(SP2)–H functionalization of aldimines and related compounds: advances and prospects, *Russ. Chem. Rev.*, 2021, vol. 90, no. 3, p. 374. https://doi.org/10.1070/RCR4978
4. Huang, B., Sun, Z., and Sun G., Recent progress in cathodic reduction-enabled organic electrosynthesis: Trends, challenges, and opportunities, *eScience*, 2022, vol. 2, no. 3, p. 243. https://doi.org/10.1016/j.esci.2022.04.006
5. Yu, Y., Yuan, Y., Liu, H., He, M., Yang, M., Liu, P., Yu, B., Dong, X., and Lei, A., Electrochemical oxidative C–H/N–H cross-coupling for C–N bond formation with hydrogen evolution, *Chem. Commun.*, 2019, vol. 55, p. 1809. https://doi.org/10.1039/C8CC09899A
6. Ali, T., Wang, H., Iqbal, W., Bashir, T., Shah, R., and Hu, Y., Electro-synthesis of organic compounds with heterogeneous catalysis, *Adv. Sci.,* 2022, vol. 9, no. 33, p. 2205077. https://doi.org/10.1002/advs.202205077

7. Novaes, L.F.T., Liu, J., Shen, Y., Lu, L., and Meinhardt, J.M., Electrocatalysis as an enabling technology for organic synthesis, *Chem. Soc. Rev.*, 2021, vol. 50, p. 7941. https://doi.org/10.1039/D1CS00223F
8. Dey, A., Gunnoe, T.B., and Stamenkovic, V.R., Organic electrosynthesis: When is it electrocatalysis, *ACS Catal.,* 2020, vol. 10, no. 21, p. 13156. https://doi.org/10.1021/acscatal.0c04559
9. Kuriganova, A.B., Lipkin, M.S., and Smirnova, N.V., Mechanism of the platinum nanoparticles formation under conditions of nonstationary electrolysis, *Mendeleev Commun.*, 2021, no. 2 (31), p. 224. https://doi.org/10.1016/j.mencom.2021.03.026
10. Faddeev, N.A., Kuriganova, A.B., Smirnova, N.V., and Leont'ev, I.N., Electrocatalytic Properties of Rh/C and Pt-Rh/C catalysts fabricated by the method of electrochemical dispersion, *Russ. J. Electrochem.,* 2019, vol. 55, p. 346. https://doi.org/10.1134/S042485701903006X
11. Kuriganova, A.B., Smirnova, N.V., and Leont'ev, I.N., PtIr/C catalysts synthesized by electrochemical dispersion method for proton exchange membrane fuel cells, *Russ. J. Electrochem.,* 2018, vol. 54. p. 561. https://doi.org/10.1134/S1023193518060113
12. Paperzh, K.O., Alekseenko, A.A., Volochaev, V.A., Pankov, I.V., Safronenko, O.A., and Guterman, V.E., Stability and activity of platinum nanoparticles in the oxygen electroreduction reaction: is size or uniformity of primary importance, *Beilstein J. Nanotechnol.*, 2021, vol. 11, p.593. https://doi.org/10.3762/BJNANO.12.49
13. Danilov, A.I., Molodkina, E.B., and Polukarov, Yu.M., Surface and subsurface oxygen on platinum in a 0.5M $H_2SO_4$ solution, *Russ. J. Electrochem.*, 2004, vol. 40, p. 585. https://doi.org/10.1023/B:RUEL.0000032007.83996.27
14. Belmesov, A.A., Baranov, A.A., Levchenko, A.V., Anodic electrocatalysts for fuel cells based on $Pt/Ti_{1-x}Ru_xO_2$, *Russ. J. Electrochem.*, 2018, vol. 54, p. 493. https://doi.org/10.1134/S1023193518060046
15. Da Silveira, G.D., Carvalho, L.M., Montoya, N., and Domenech-Carbo, A., Solid state electrochemical behavior of organosulfur compounds, *Electroanalyt. Chem.,* 2017, vol. 806, p.180. https://doi.org/10.1016/j.jelechem.2017.10.055
16. Jia, H., Xu, Y., Zou, L., Gao, P., Zhang, X., Taing, B., Matthews, B.E., Engelhard, M.H., Burton, S.D., Han, K.S., Zhong, L., Wang, Ch., and Xu, W., Sulfone-based electrolytes for high energy density lithium-ion batteries, *J. Power Sources,* 2022, vol. 527, p. 231171. https://doi.org/10.1016/j.jpowsour.2022.231171
17. Gafurov, M.M., Rabadanov, K.S., Ataev, M.B., Aliev, A.R., Ahmedov, I.R., Kakagasanov, M.G., and Kraminin, S.P., Vibrational spectra of an $LiNO_3$–$(CH_3)_2SO_2$ system, *JAS*, 2012, no. 2 (79), p. 184. https://doi.org/10.1007/s10812-012-9581-7
18. Markaryan, Sh.A., Aznauryan, M.G., and Kazoyan, E.A., Physicochemical properties of aqueous solutions of dimethyl- and diethylsulfones, *Russ. J. Phys. Chem.,* 2011, no. 12 (85), p. 2138. https://doi.org/10.1134/S0036024411120211
19. Kolosnitsyn, V.S., Kostryukova, N.V., and Legostaeva, M.V., Electrical conductivity and thermal properties of gel polymer electrolytes based on sulfones, *Elektrokhim. Energ.*, 2004, no. 2 (4), p. 90.
20. Kang, S., Jeon, B., Hong, S.-T., and Lee, H., A sulfone-based crystalline organic electrolyte for 5 V solid-state potassium batteries, *Chem. Eng. J.,* 2022, vol. 443, p. 136403. https://doi.org/10.1016/j.cej.2022.136403
21. Wu, W., Bai, Y., Wang, X., and Wu, C., Sulfone-based high-voltage electrolytes for high energy density rechargeable lithium batteries: Progress and perspective, *Chin. Chem. Lett.,* 2021, no. 4 (32), p. 1309. https://doi.org/10.1016/j.cclet.2020.10.009
22. Terent'ev, A.O., Mulina, O.M., Ilovaisky, A.I., Kokorekin, V.A., and Nikishin, G.I., Ammonium iodide-mediated electrosynthesis of unsymmetrical thiosulfonates from arenesulfonohydrazides and thiols, *Mendeleev Commun.*, 2019, vol. 29, p. 80. https://doi.org/10.1016/j.mencom.2019.01.027
23. Terent'ev, A.O., Mulina, O.M., Pirgach, D.A., Demchuk, D.V., Syroeshkin, M.A., and Nikishin, G.I., Copper (I)-mediated synthesis of β-hydroxysulfones from styrenes and sulfonylhydrazides: an electrochemical mechanistic study, *RSC Adv.*, 2016, vol. 6, p. 93476. https://doi.org/10.1039/C6RA19190H
24. Terent'ev, A.O., Mulina, O.M., Pirgach, D.A., Ilovaisky, A. I., Syroeshkin, M.A., Kapustina, N.I., and Nikishin, G.I., Electrosynthesis of vinyl sulfones from alkenes and sulfonyl hydrazides mediated by KI: An electrochemical mechanistic study, *Tetrahedron*, 2017, vol.73, p. 6871. https://doi.org/10.1016/j.tet.2017.10.047
25. Park, J.K. and Lee, S., Sulfoxide and sulfone synthesis via electrochemical oxidation of sulfides, *J. Org. Chem.*, 2021, no. 19 (86), p. 13790. https://doi.org/10.1021/acs.joc.1c01657
26. Krtil, P., Kavan, L., Hoskovcová, I., and Kratochvilová, K., Anodic oxidation of dimethyl sulfoxide based electrolyte solutions: An in situ FTIR study, *J. Appl. Electrochem.,* 1996, vol. 26, p. 523. https://doi.org/10.1007/BF01021976
27. Akhmedov, M.A., Khidirov, Sh.Sh., and Kaparova, M.Yu., Electrochemical oxidation of dimethyl sulfone in alkaline medium, *Izv. Vyssh. Uchebn. Zaved., Khim. Khim. Tekhnol.,* 2018, vol. 61, no. 8, p. 32. https://doi.org/10.6060/ivkkt.20186108.5707
28. Khidirov, Sh.Sh., Akhmedov, MA, Rabadanov, M.Kh., and Kaparova, M.Y., Russian Patent 2641302, 2018. https://goo-gl.su/mHzIEP
29. Akhmedov, M.A., Khidirov, Sh.Sh., Kaparova, M.Y., and Khibiev, Kh.S., Electrochemical synthesis of methanesulfonic acid from aqueous solutions of dimethyl sulfone, *Izv. Vyssh. Uchebn. Zaved., Khim. Khim. Tekhnol.,* 2016, no. 12 (59), p. 100. https://doi.org/10.6060/tcct.20165912.5345
30. Akhmedov, M.A. and Khidirov, Sh.Sh., Anodic processes at smooth platinum electrode in concentrated solution of methanesulfonic acid, *Russ. J. Electrochem.,* 2019, vol. 55, p. 579. https://doi.org/10.1134/S1023193519060028

31. Khidirov, Sh.Sh., Akhmedov, M.A., and Rabadanov, M.Kh., Russian Patent 2554880, 2015. https://goo-gl.su/L0WTTTz

32. Khidirov, Sh.Sh. Akhmedov, MA, Khibiev, Kh.S., and Omarova, K.O., Russian Patent 2496772, 2013. https://goo-gl.su/5WOgLhxS

33. Akhmedov, M.A., Ibragimova, K.O., and Khidirov, Sh.Sh., Comparative evaluation of dimethylsulfoxide and dimethyl sulfone adsorption on a smooth platinum electrode in acidic, *Russ. J. Electrochem.,* 2020, vol. 56, p. 396. https://doi.org/10.1134/S1023193520040023

34. Trasatti, S. and Petrii, O.A., Real surface area measurements in electrochemistry, *J. Electroanalyt. Chem.,* 1992, vol. 327, p. 353. https://doi.org/10.1016/0022-0728(92)80162-w

35. *Electroanalytical Methods. Guide to Experiments and Applications,* Scholz, F., Ed., Heidelberg: Springer, 2010.

36. Budnikov, G.K., Maistrenko, V.N., and Vyaselev, M.R., *Osnovy sovremennogo elektrokhimicheskogo analiza* (Fundamentals of Modern Electrochemical Analysis), Moscow: Mir, Binom LZ, 2003.

37. Brandenburg, J. G., Bannwarth, C., Hansen, A., and Grimme, S., B97-3c: A revised low-cost variant of the B97-D density functional method, *J. Chem. Phys.,* 2018, no. 6(148), p. 064104. https://doi.org/10.1063/1.5012601

38. Neese, F., Wennmohs, F., Becker, U., and Riplinger, C., The ORCA quantum chemistry program package, *J. Chem. Phys.,* 2020, vol. 152, p. 224108. https://doi.org/10.1063/5.0004608

39. Neese, F. Software update: The ORCA program system—Version 5.0, *WIREs Comput. Mol. Sci.,* 2022, p. e1606. https://doi.org/ bbb https://doi.org/10.1002/wcms.1606

40. Perdew, J.P., Burke, K., and Ernzerhof, M., Generalized gradient approximation made simple, *Phys. Rev. Lett.,* 1996, vol. 77, p.3865. https://doi.org/10.1103/PhysRevLett.77.3865

41. Hellweg, A. and Rappoport, D., Development of new auxiliary basis functions of the Karlsruhe segmented contracted basis sets including diffuse basis functions (def2-SVPD, def2-TZVPPD, and def2-QVPPD) for RI-MP2 and RI-CC calculations, *Phys. Chem. Chem. Phys.* 2015, vol. 17, p.1010. https://doi.org/10.1039/C4CP04286G

42. Weigend, F. and Ahlrichs, R., Balanced basis sets of split valence, triple zeta valence and quadruple zeta valence quality for H to Rn: Design and assessment of accuracy, *Phys. Chem. Chem. Phys.,* 2005, vol. 7, p.3297. https://doi.org/10.1039/B508541A

43. Marenich, A.V., Cramer, C.J., and Truhlar, D.G., Universal solvation model based on solute electron density and on a continuum model of the solvent defined by the bulk dielectric constant and atomic surface tensions, *J. Phys. Chem. B,* 2009, vol. 113, p.6378. https://doi.org/10.1021/jp810292n

44. Van Spronsen, M.A., Frenken, J.W.M., and Groot, I.M.N., Observing the oxidation of platinum, *Nat. Commun.*, 2017, vol. 8, p. 429. https://doi.org/10.1038/s41467-017-00643-z

45. Akhmedov, M.A. and Khidirov, Sh. Sh., Electrocatalytic oxidation of ethanol on the platinum electrode in solution of methanesulfonic acid, *Russ. J. Electrochem.,* 2022, vol. 58, p. 482.] https://doi.org/10.1134/S1023193522060039

46. Halseid, R., Bystroň, T., and Tunold, R., Oxygen reduction on platinum in aqueous sulphuric acid in the presence of ammonium, *Electrochim. Acta,* 2006, no. 13 (51), p.2737. https://doi.org/10.1016/j.electacta.2005.08.011

47. Wongbua-ngam, P., Veerasai, W., Wilairat, P., and Kheowan, O.-U., Model interpretation of electrochemical behavior of Pt/H2SO4 interface over both the hydrogen oxidation and oxide formation regions, *Int. J. Hydrogen Energy,* 2019, no. 23 (44), p.12108. https://doi.org/10.1016/j.ijhydene.2019.03.076

48. Santosh, K.C. and Abolfath, R., Towards the ionizing radiation induced bond dissociation mechanism in oxygen, water, guanine and DNA fragmentation: a density functional theory simulation, *Sci. Rep.,* 2022, vol. 12, p.19853. https://doi.org/10.1038/s41598-022-23727-3

49. Pentin, Yu.A. and Kuramshina, G.M., *Osnovy molekulyarnoi spektroskopii* (The fundamentals of molecular spectroscopy), Moscow: Mir, 2008.

50. Müller, J.F., Liu, Z., Nguyen, V., Stavrakou, T., Harvey, J. N., and Peeters, J., The reaction of methyl peroxy and hydroxyl radicals as a major source of atmospheric methanol, *Nat. Commun.*, 2016, vol.7, p.13213. https://doi.org/10.1038/ncomms13213

51. Toffel, P. and Henglein, A., Polarogram of the free hydrogen atom and of some simple organic radicals, *Discuss. Faraday Soc.*, 1977, vol. 63, p. 124. https://doi.org/10.1039/DC9776300124

52. Kurmaz, V.A., Kotkin, A.S., and Simbirtseva, G.V., Laser photoemission generation and electrochemical study of methyl radicals as secondary products of OH radicals capture by dimethyl sulfoxide molecules, *J. Solid State Electrochem.*, 2011, vol. 15, p. 2119. https://doi.org/10.1007/s10008-011-1534-1

53. Bockris, J.O.M., Ammar, I.A., and Huq, A.K.M.S., The mechanism of the hydrogen evolution reaction on platinum, silver and tungsten surfaces in acid solutions, *J. Phys. Chem.,* 1957, no. 7 (61), p. 879. https://doi.org/10.1021/j150553a008

54. Fang, Y.-H., Wei, G.-F., and Liu, Z.-P., Catalytic role of minority species and minority sites for electrochemical hydrogen evolution on metals: surface charging, coverage, and Tafel kinetics, *Phys. Chem. C,* 2013, vol. 117, p.7669. https://doi.org/10.1021/jp400608p

55. Rheinländer, P.J., Herranz, J., Durst, J., and Gasteiger, H.A., Kinetics of the hydrogen oxidation/evolution reaction on polycrystalline platinum in alkaline electrolyte reaction order with respect to hydrogen pressure, *J. Electrochem. Soc.*, 2014, vol. 161, p. F1448. https://doi.org/10.1149/2.0501414jes

*Translated by T. Safonova*